



**INTERNATIONAL FOOD
POLICY RESEARCH INSTITUTE**
sustainable solutions for ending hunger and poverty
Supported by the CGIAR

IFPRI Discussion Paper 00867

May 2009

Joint Water Quantity/Quality Management Analysis in a Biofuel Production Area

Using an Integrated Economic-Hydrologic Model

Márcia Maria Guedes Alcoforado de Moraes

Ximing Cai

Claudia Ringler

Bruno Edson Albuquerque

Sérgio P. Vieira da Rocha

Carlos Alberto Amorim

Environment and Production Technology Division

INTERNATIONAL FOOD POLICY RESEARCH INSTITUTE

The International Food Policy Research Institute (IFPRI) was established in 1975. IFPRI is one of 15 agricultural research centers that receive principal funding from governments, private foundations, and international and regional organizations, most of which are members of the Consultative Group on International Agricultural Research (CGIAR).

FINANCIAL CONTRIBUTORS AND PARTNERS

IFPRI's research, capacity strengthening, and communications work is made possible by its financial contributors and partners. IFPRI receives its principal funding from governments, private foundations, and international and regional organizations, most of which are members of the Consultative Group on International Agricultural Research (CGIAR). IFPRI gratefully acknowledges the generous unrestricted funding from Australia, Canada, China, Finland, France, Germany, India, Ireland, Italy, Japan, Netherlands, Norway, South Africa, Sweden, Switzerland, United Kingdom, United States, and World Bank.

AUTHORS

Márcia Maria Guedes Alcoforado de Moraes, Universidade Federal de Pernambuco, Brazil

Adjunct Professor, Department of Economics

marciagamoraes@yahoo.com.br

Ximing Cai, University of Illinois at Urbana-Champaign

Assistant Professor, Department of Civil and Environmental Engineering

Claudia Ringler, International Food Policy Research Institute

Senior Research Fellow, Environment and Production Technology Institute

Bruno Edson Albuquerque, Universidade Federal de Pernambuco, Brazil

Fellow, CT-Hidro/ FINEP/ CNPq funded research project, Department of Economics

Sérgio P. Vieira da Rocha, Universidade Federal de Pernambuco, Brazil

Fellow, CT-Hidro/FINEP/ CNPq funded research project, Department of Economics

Carlos Alberto Amorim, Universidade Federal de Pernambuco, Brazil

Master Student, Economics

Notices

¹ Effective January 2007, the Discussion Paper series within each division and the Director General's Office of IFPRI were merged into one IFPRI-wide Discussion Paper series. The new series begins with number 00689, reflecting the prior publication of 688 discussion papers within the dispersed series. The earlier series are available on IFPRI's website at www.ifpri.org/pubs/otherpubs.htm#dp.

² IFPRI Discussion Papers contain preliminary material and research results, and have been peer reviewed by at least two reviewers—internal and/or external. They are circulated in order to stimulate discussion and critical comment.

Contents

Abstract	v
Abbreviations And Acronyms	vii
1. Background	1
2. Methodology	4
3. Analysis of Results	13
4. Conclusions	20
References	21

List of Tables

Table 1. Submodel 1 water allocation results under low-flow scenario (60% of average flows)	13
---	----

List of Figures

Figure 1. Location of the State of Pernambuco and the Pirapama River Basin as well as the first stretch of the basin where the model is applied	1
Figure 2. The node-link network of the Pirapama basin model	2
Figure 3. Relationships between DO curves and critical times, (a) $tc > 0$, (b) $tc = 0$, (c) $tc < 0$	9
Figure 4. Actual and fertirrigated areas compared with modeled areas in the submodel with 60 percent of normal hydrology (dry scenario)	14
Figure 5. Fertirrigated areas for JB in submodel 1 and the full model.	15
Figure 6. Fertirrigated areas as a share of total area in node FI7, full model	16
Figure 7. BOD loads in thousands of Kg BOD/day, site FI7, full model	16
Figure 8. Water allocation for Vitória resulting from the submodel and full model and water use right (=flow demand).	17
Figure 9. BOD loads with the full model for fertirrigated sites: FI5, FI5_1, FI6, and FI7	18
Figure 10. Águas Claras reservoir storage from the submodel and full model	19
Figure 11. Flow release from Águas Claras reservoir under the submodel and the full model	19
Figure 12. Shadow-price on the limit of phosphorus for Águas Claras reservoir, full model	19

ABSTRACT

Water management in the Pirapama River Basin in northeastern Brazil is affected by both water quantity and water quality constraints. The region is known for significant sugarcane-based ethanol production—which is key to the Brazilian economy and expected to grow dramatically under recent global changes in energy policy. Sugarcane production in the region goes hand in hand with controlled fertirrigation practices with potentially significant adverse impacts on the environment. To assess sustainable water allocation in the basin, an integrated hydrologic-economic basin model is adapted to study both water quantity and water quality aspects. The model results show that incorporating water quality aspects into water allocation decisions leads to a substantial reduction in application of vinasse to sugarcane fields. To enforce water quality restrictions, the shadow price for maintaining water in the reservoir could be used as a pollution tax for fertirrigated areas, which are currently not subject to pollution charges.

Key Words: water quality, river basin management, integrated economic-hydrologic modeling, nonlinear optimization, biofuel

ABBREVIATIONS AND ACRONYMS

RMR	Pirapama River Basin
BOD	biochemical oxygen demand
DO	dissolved oxygen
GAMS	General Algebraic Modeling System
CONAMA	Conselho Nacional do Meio Ambiente
SCH	small central hydroelectric

1. BACKGROUND

The Pirapama River Basin is located in the metropolitan regions of Recife – locally known as RMR – and the Pernambuco Mata, in northeastern Brazil (see Figure 1). It covers an area of about 600 square kilometers, and the approximate length of its main waterway is 80 kilometers. The Pirapama is the most important water source for the city of Recife, capital of the state of Pernambuco. The region is affected by lack of adequate water and sewage treatment, resulting in high levels of water pollution during dry spells (Ribeiro 2000). Throughout the length of the river, most of the currently monitored water quality standards cannot be met. To resolve domestic water supply problems, two reservoirs have been planned, one on the Águas Claras tributary and one on the Pirapama mainstream. The latter reservoir is almost completed (Figure 2). Although these reservoirs might reduce the incidence of dry spells, they might also contribute to further water quality deterioration through eutrophication processes. Water quality in the Pirapama was assessed during 1990–1996 within the scope of the Pirapama Project (DFID and CPRH 1999), which was drawn up by the RMR to propose regulations to minimize the conflicts among economic growth, environmental management, and social development in the basin. According to that assessment, total phosphorous displayed worrying levels even before the construction of the Pirapama reservoir. The largest source of water pollution in the first part of the basin is sugarcane production together with fertirrigation. Fertirrigation is a joint process of irrigation and fertilization that uses irrigation water to carry and distribute fertilizers to crops. In the context of sugarcane production, the focus is on the amount of potassium carried by the vinasse and transferred to the soil.

Figure 1. Location of the State of Pernambuco and the Pirapama River Basin as well as the first stretch of the basin where the model is applied

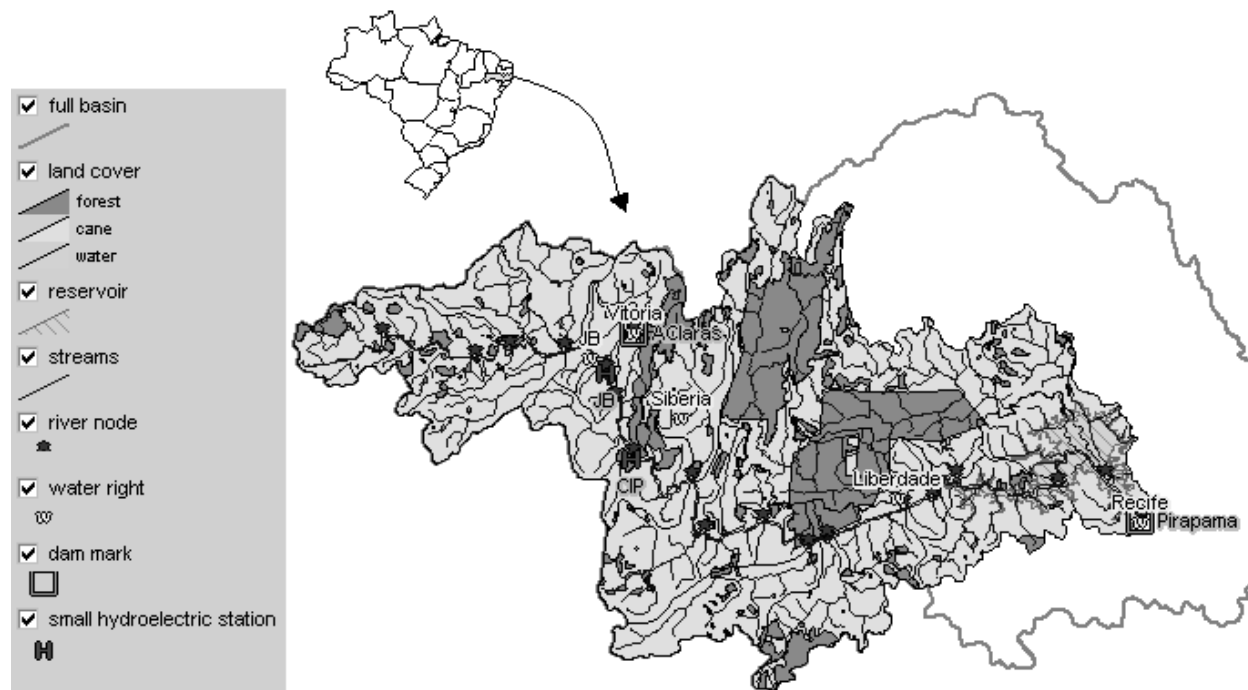
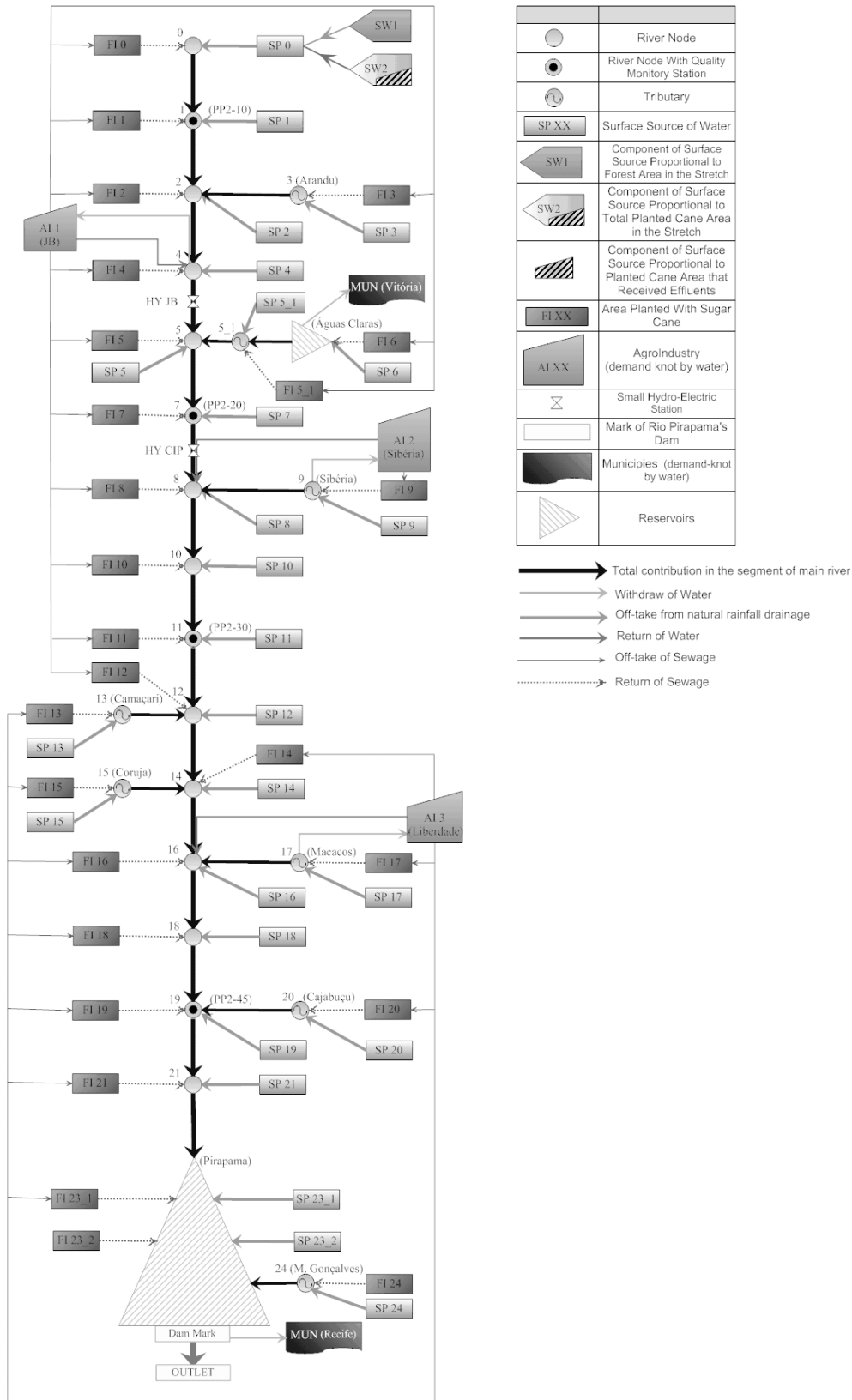


Figure 2. The node-link network of the Pirapama basin model



Brazil is the world's largest ethanol producer, and the sugar-alcohol sector in Brazil is responsible for 21 percent of GNP and about 14 percent of formal employment. Given energy security and climate change concerns in Brazil and elsewhere, production is expected to continue to expand rapidly over the next several years. To reduce adverse environmental impacts of commercial sugarcane plantations and industry in the country, discharge of effluents with high organic loads has been replaced with controlled fertirrigation practices of vinasse; there are efforts to preserve riparian forests; harvest burning is being phased out; and the rate of water reutilization in sugar mills has increased. Vinasse can entirely replace the fertilization that uses potassium and sulfur and partially replace fertilization with nitrogen, a fact that is economically interesting because fertilization with potassium is carried out through the use of potassium chloride (KCl), which is costly. Today Brazil has about 0.65 million hectares of fertirrigated areas, which corresponds to 12 percent of the area cultivated with cane (International Sugarcane Biomass Utilization Consortium 2007). According to government regulations, vinasse application is restricted to 450 cubic meters per hectare (m^3/ha) for direct juice vinasse, 300 m^3/ha for blended juice vinasse, and 150 m^3/ha for molasses vinasse given that the application of vinasse for long periods may adversely affect both soil micronutrients and groundwater resources (Ludovice et al. 2005).

This study will focus on the first stretch of the river basin from the source to the Pirapama reservoir. This river reach is of crucial importance, because most of the agroindustries—chiefly sugarcane distilleries—in the basin are located in this area and therefore most of the organic effluent load is generated in this reach and subsequently transported into the reservoir. Among the factors that have led to the occurrence of pollution in the stretch, the most significant one is the presence of sugarcane residue of three alcohol distilleries: JB, Sibéria, and Liberdade. The ethanol production from the industries (distilleries) at the time when the Integrated Diagnostic study was drawn up (Gama 1998) was about 94,000 m^3/year , or 522,000 liters/day. The cane residue of these industries has a potential organic load of 226,335 kg biochemical oxygen demand (BOD)/day that is equivalent to the load from an urban area with a population of around 4.2 million (calculated based on a load of 54 g/habitant/day for BOD in domestic sewage; see also Von Sperling 1996).

To assess sustainable water allocation in the RMR, a model that integrates essential relationships of hydrology, water quality, and economics at the river basin scale is adopted to study both water quantity and water quality aspects. The model is used to estimate the impact on the marginal value of water uses and water allocation from the restriction of total BOD and DO (dissolved oxygen) at a certain level. Through the modeling analysis, this paper demonstrates the policy implications of integrated water quantity and quality management in the content of a river basin with heavy biomass and biofuel production.

The following sections discuss the methodology of the model, including both water quantity and quality submodels; discuss the implications of water quality restrictions for reservoir operation; and describe management options, including compensation schemes, allocations, treatment, and distribution.

2. METHODOLOGY

Overview of the River Basin Model

The methodology used is an integrated hydrologic-agronomic-economic river basin model based on Cai et al. (2006) extending the methodology to combined water quantity and quality management. Previous models incorporated salinity in the irrigation water (Cai et al. 2003, 2006) but not BOD or DO, which require more complex functional forms. The model was developed at the Federal University of Pernambuco (Moraes 2003) in a partnership between the Hydraulics Laboratory and the Department of Economics and was funded by Brazilian government agencies. The model is built using the General Algebraic Modeling System (GAMS) and is implemented using the piece-by-piece approach presented in Cai et al. (2001) with a sequential implementation of the quantity and quality submodels.

The quality submodel allows the restriction of effluents to government-mandated levels and the calculation of pollution levels that limit atrophy in reservoirs. Thus, the model not only deals with the question of optimal water (quantity) allocation, but also the question of quality. Joint water quantity/quality modeling is critical for the Pirapama, considering reservoir storage and release policy has already affected the water quality in the river, but also for other Brazilian river basins with large sugarcane plantations given the rapid growth in demand for sugarcane as feedstock for bioethanol.

Model Structure

Hydrologic and Economic Relationships

The model contains a large number of physical and economic relationships and allocation decisions at various scales. At the basin level, water allocation among various demand sites and sectors is carried out. At the individual system level, the optimal quantity and timing for effluent application among sugarcane areas are determined. Eight major tributaries are simulated as well as other major inflow sources, including water for refrigeration released by the agroindustries (shown as returns of water in Figure 2). These water quantities are listed in the operating licenses of the agroindustries approved by the government, but no data are available regarding the quality of this source. Rainfall/runoff is accounted for in the model by dividing the sub-basin into several geographic areas, including forest and sugarcane areas, with differing runoff coefficients. Water withdrawals are determined based on existing concessions, which are granted by the Secretary for Water Resources at withdrawal levels above 48 m³/day.

Net benefits are determined for all uses considered in the model including domestic supply (municipalities of Recife and Vitória), industrial supply (the JB, Sibéria, and Liberdade agroindustries), hydropower generation (Small Hydropower Station *Destilaria JB* [SHSJB] and Small Hydropower Station *Companhia Industrial Pirapama* [SHSCIP]), and fertirrigation. Inverse demand functions, assuming that elasticities are constant along the demand curve (see Moraes et al. 2006), are determined for each of these water uses based on obtained values of price elasticities of the demand for water at various offtake points (Carrera-Fernandez 1999). Monthly gross benefits are calculated by integrating the inverse demand functions to allocated values. Net benefits for domestic supply and electricity generation are determined as follows:

$$B(U, t) = \left| \frac{P_0}{-Q_0} \right|^\varepsilon \cdot \left[\frac{Q_0^{\varepsilon+1}}{\varepsilon+1} - \frac{|Q_0 - Q_a(U, t)|^{\varepsilon+1}}{\varepsilon+1} \right] - CW * Q_a(U, t) \quad (1)$$

where P_0 is the price in the inverse demand function with zero water use; Q_0 is the quantity allocated associated with a (close to) zero value and Q_a is the actual water allocated; ε ($=1/\eta$) is the

inverse of the demand price-elasticity (η); CW is the delivery cost of water for electricity or domestic supply; U stands for user.¹

Net benefits for agroindustrial supply include an effluent surplus cost. The variable, which measures the effluent surplus produced by each agroindustry and in each month, is both a function of monthly water allocation to that industry (as this decision will affect the total quantity of effluents produced), and a function of monthly vinasse allocation to fertirrigated areas. Fertirrigation incorporates both transport costs and savings of fertilizer applications.

Fertirrigation is a joint process of irrigation and fertilization that uses irrigation water to carry and distribute fertilizers to crops. In the benefit function of fertirrigation the decision variable is the quantity of area fertirrigated, here A_a (using a constant rate of effluent application of 300 m³/ha). Allocation above the maximum effluent, equal to the constant rate of effluent application, has zero value. CW is the cost of applying the effluent (aspersión) per hectare. To determine fertilizer application savings we added a term in the benefit function of R\$267.15/ha or US\$100/ha, G_{medio} , which reflects the average savings. Transport costs consider the volume transported and the distance. Thus, the benefit function for fertirrigation is

$$B(U, t) = \left| \frac{P_0}{-A_0} \right|^\varepsilon \cdot \left[\frac{A_0^{\varepsilon+1}}{\varepsilon+1} - \frac{|A_0 - A_a(U, t)|^{\varepsilon+1}}{\varepsilon+1} \right] - CW * A_a(U, t) + G_{medio} * A_a(U, t) - C_{transp}(U, t) \quad (2)$$

The objective function then maximizes the net benefits to the basin as follows:

$$Obj = \sum_{mun} Bm(Um) + \sum_{aind} Bi(Ui) + \sum_{pch} Be(Ue) + \sum_{frrig} Bf(Uf) \quad (3)$$

where $Bm(Um)$, $Bi(Ui)$, $Be(Ue)$ and $Bf(Uf)$ are the sum of annual net benefits from water use in the municipality, industry, hydropower generation, and fertirrigation. Additional details for these subfunctions are found in Moraes et al. (2006).

Water allocation is subject to a series of hydrological (water quantity and quality) and institutional constraints. Hydrologic constraints include mass balances of water quantity at river reaches, reservoirs, and water demand sites (see Cai et al. 2003, 2006 for details). Institutional constraints include effluent application limits, which have been described in Section 1. These are determined based on area planted with sugarcane by month and location, and the volume of vinasse applied.

Water Quality Modeling

An assessment of water quality in the Pirapama River was carried out under Project Pirapama between 1990 and 1996. Results showed that BOD, DO, and fecal coliform levels were significantly above government-mandated pollution levels. The study identified fertirrigation with sugarcane residues as the main pollutant (Gama 1998).

To assess the environmental impact of fertirrigation, Moraes (2003) developed a water quality simulation model based on the Streeter-Phelps equations (Streeter and Phelps 1925). The model simulates constituent decomposition (BOD and DO) with highly nonlinear equations. Constituents are a measure of the pollution level from the main sources of contamination (vinasse, herbicides, and pesticides from sugarcane production) in the first stretch of the river. The vinasse produced in the study area is currently deposited on sugarcane fields through fertirrigation. The residues can reach the water bodies through runoff during fertirrigation application, underground seepage or runoff during rainfall events. Another source of pollutant load is leakage from ponds that store the effluent surplus, which is not applied in the

¹ Regarding electricity production, the maximum flow associated with maximum plant capacity (Q_0) is 1.57 m³/sec for 0.96 MW (Megawatt) for the SHSJB plant and 4.35 m³/sec for 1.85 MW for the SHSCIP plant. The head of the stations is 73 and 51 meters, respectively, and production efficiency is 85% for both stations.

fertirrigation process. The results of the simulation model show that this type of leakage is important for explaining the BOD and DO levels in 2000 and 2001. Leakage from ponds was considered in the simulation model to calibrate the parameters. However, pond leakage was not included in the optimization because it is not considered a management option.

Nonpoint pollution was simulated at a monthly time-step at river flow intakes corresponding to the various drainage areas. The model was validated through comparing the model output with values measured along the river (see river nodes with quality gauging stations in Figure 2).

Currently, there are no pollution charges for the fertirrigation process. The model presented here can be used to develop economic incentives based on estimates of nonpoint source pollution loads from the crop fields under fertirrigation, which can be compared to an even worse case, effluent discharge directly to the water bodies, and a better case, some form of treatment of the effluent discharge.

At each node the incoming pollution concentrations of mixed inflows are calculated as the flow rate-weighted average. After the concentrations of the constituents are determined at each node, the autodepuration process can be simulated for the next river segment through the application of decomposition equations, which depend on the physical characteristics of the segment as well as on the initial concentration. In the case of BOD, the constituent refers to the amount of oxygen required to stabilize the carbonaceous organic material through biochemical processes. To calculate BOD at the end of the river stretch it is necessary to use the concept of remaining BOD, which gives the concentration of remaining organic material in net mass at a given moment (Von Sperling 1996) and is calculated as follows:

$$L_t = L_0 e^{-K_1 t} \quad (4)$$

where L_0 is the remaining BOD at $t=0$ (mg/l), L_t is the remaining BOD at the end of any other time t (mg/l), and K_1 is the coefficient of deoxygenation (day^{-1}), which represents the rate at which the consumption of oxygen progresses over time. The coefficient depends on the characteristics of the organic matter, in addition to temperature and the presence of inhibiting substances. The effluents considered here are cane residues from fertirrigation and fertilizers. Reference values for the coefficient of deoxygenation of these effluents were not found; given that these constituents have high degradation rates, we used the highest value presented in a table of typical values for K_1 adapted by Von Sperling (1996), which is 0.45 day^{-1} .

Therefore, the remaining BOD at the end of each segment in each month is given by:

$$BOD(n, m) = BOD_0(n, m) e^{-K_1 t(n, m)} \quad (5)$$

where t is the travel time in segment n and in month m , which depends on the length of the river stretch, the size of the river transaction, and the velocity of flow (Loucks et al. 1967). To consider the worst case of water quality, we use the minimum daily flow during a month rather than the average monthly flow to simulate the autodepuration process. Thus, while we model monthly flows, these are aggregated from daily flows, using the minimum daily flow in a month. The velocity of flow depends on the flow rate; we used the minimum daily flow during a month.

To determine the minimum daily flow in the optimization model, we assume a linear relationship between the average monthly flow and the minimum daily flow, and the ratio between the two is based on the observation in the base year, 2004. Thus, the average monthly flow is determined by the optimization model as a decision variable, and the minimum daily flow is calculated as a fraction of the average monthly flow.

The BOD at the end of one reach is then used as the entry of the next reach to calculate BOD along the river. DO is simulated similarly to BOD by calculating the level of DO at the start and end of each reach in each month, considering the various sources such as effluent discharges, return flows, and runoffs.

Since the various sources of DO are mixed at some river nodes, the concentration calculated as the flow-weighted average over all sources can be higher than the saturation level. If this occurs, the concentration is set equal to the saturated concentration. The saturation concentration of DO (DO_{sat}) is obtained from measurements at quality stations. For those river reaches and tributaries without gauging stations, DO_{sat} is estimated using a functional form taking into account temperature and altitude (Von Sperling 1996).

The DO value at the end of each river stretch is obtained through the Streeter-Phelps equation, which expresses the DO concentration after the elapse of any time t with an initial discharge at $t=0$, based on various physical characteristics that determine the capacity for depuration:

$$DO_t = DO_{sat} - \left[\frac{K_1}{(K_2 - K_1)} * BOD_0 * (e^{-K_1 t} - e^{-K_2 t}) + (DO_{sat} - DO_0) * e^{-K_2 t} \right] \quad (6)$$

where DO_{sat} and K_1 (the coefficient of deoxygenation [day^{-1}]) are related to the physical characteristics of the river at that point as well as to the effluents discharged. K_2 is the coefficient of reaeration, which represents the rate of absorption of oxygen within the process of atmospheric reaeration, which occurs by means of the gaseous exchanges in the interface gas-liquid. The value of this coefficient depends on the depth and velocity of the watercourse or river flow. For this analysis, tabled values (Von Sperling 1996) related to velocities are used. The velocity of each stretch and month is obtained from the cross-section area and the minimum flow in the month rather than the average, as stated before. The value of this coefficient has a greater influence in the results of the balance of DO than K_1 , due to its wider range of variation. $(DO_{sat} - DO_0)$ is the initial deficit of oxygen after mixing and is a function of the prior situation of the river and of the discharge where DO_0 is the initial concentration of oxygen after mixing. BOD_0 is the BOD resulting after mixing. Based on equation (6) the final DO values are calculated. If the DO value is negative, which is mathematically possible, the simulation will substitute the result with zero.

Based on these equations, observed 2000 values were first used to calibrate the remaining unknown values. Values for 2001 were then modeled and compared with 2001 observed data for model validation. The results of the simulation model showed that the Streeter-Phelps simplified model for water quality was appropriate for the case study.

In the optimization model several additional constraints were included for water quality modeling. First, the minimum value of DO concentration is met along the watercourse. The DO concentration is calculated for all river reaches. The minimum DO value relates to the form of the DO curve and the concept of critical time (Von Sperling 1996). The formula of critical time is derived from the formulation, which relates the status of DO over time (see equation 6), and is given by

$$t_c = \frac{1}{K_2 - K_1} * \ln \left(\frac{K_2}{K_1} \left[1 - \frac{(DO_{sat} - DO_0)(K_2 - K_1)}{BOD_0 K_1} \right] \right) \quad (7)$$

where the terms have the same meaning as in equation (6). The concentration associated with the critical time is called the critical concentration and is represented by (Von Sperling 1996)

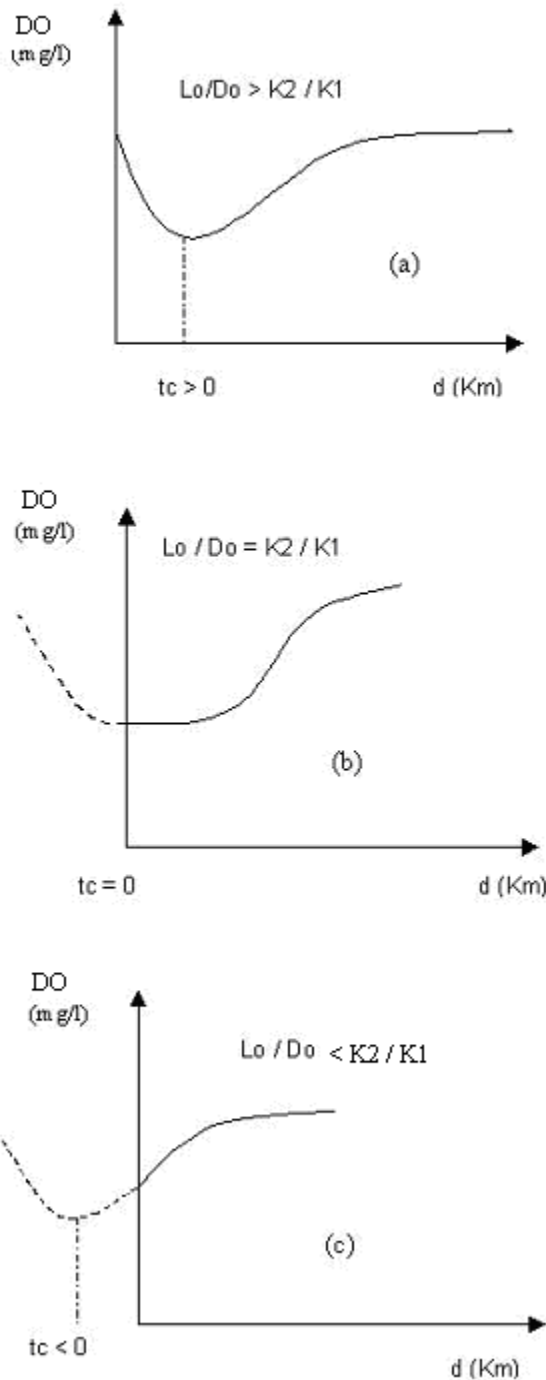
$$DO_c = DO_{sat} - \frac{K_1}{K_2} * BOD_0 * e^{-K_1 t_c} \quad (8)$$

To ensure that the lowest admissible DO level is adopted not only at the starting and ending nodes of a river stretch but also throughout the entire stretch, the relationship between the ratios $BOD_0 / (DO_{sat} - DO_0)$ and K_2 / K_1 is used, as shown in Figure 3, where $Lo = BOD_0$ and $D_0 = DO_{sat} - DO_0$. For case (a) with $t_c > 0$, the critical time must be calculated and compared with the size of the stretch in the month. If the critical time is less than the time for water to run through the segment

(travel time), a lower DO concentration may occur in the middle of the segment. Under this situation, the load, which depends on water and effluent allocation, is limited to DO_{crit} greater than or equal to 5 milligrams per liter (mg/l), the minimum value established by the governmental quality regulation agency (Conselho Nacional do Meio Ambiente [CONAMA]) for domestic and other uses (Gama 1998) and applicable for this river. This limitation is obtained by rearranging equation (8) as an inequality equation, as follows:

$$\frac{K_1}{K_2} * BOD_0 * e^{-K_1 t_c} \leq DO_{sat} - 5 \quad (9)$$

Figure 3. Relationships between DO curves and critical times, (a) $t_c > 0$, (b) $t_c = 0$, (c) $t_c < 0$



Note: $L_0 = BOD_0$, $D_0 = DO_{sat} - DO_0$.

For the second situation, the critical time is greater than the total travel time, which implies that the critical concentration will not be attained within the stretch. In that case, the DO at the end of the stretch must be set to be greater than the admissible limit (5 mg/l), because the critical situation will not occur inside the stretch. In order to obtain the load limitation, which ensures the admissible DO level for

the entire stretch, equation (6) must be rearranged to recalculate the DO at the end of time t , which results in equation (10):

$$\frac{K_1}{(K_2 - K_1)} * BOD_0 * (e^{-K_1 t} - e^{-K_2 t}) + (DO_{sat} - DO_0) * e^{-K_2 t} \leq DO_{sat} - 5 \quad (10)$$

In cases (b), $t_c=0$, and (c), $t_c < 0$ (see Figure 3), we can consider in practical terms that the critical time is zero and the lowest value occurs at the initial point. Note that if we can assure that DO_{crit} is greater than or equal to 5 mg/l (see equation 9) then both DO_0 and DO at the end of the river reach (as can be seen from the shape of the curve) will also be greater or equal to 5 mg/l.

The most significant contributor to river loads is from residues in the area planted with sugarcane associated with the previous stretch. Depending on the area fertirrigated, the area of cane that receives only fertilizers, and on the wooded areas, runoff contributes BOD levels in the range of 1–30 mg/l, respectively. Moreover the coefficient of reaeration (K_2), as well as the travel time, are functions of the runoff and can influence pollutant levels in river stretches. During optimization, the medium flow in each stretch and month is a decision variable. Thus, the water quality module reallocates water and cane residue to satisfy water quality standards.

Since the Streeter-Phelps equations cannot be used to load discharge in reservoirs, a separate constraint is included. In order to characterize the eutrophication stage of a water body, various degrees of atrophy can be distinguished, including *oligotrophic* for clear lakes with low productivity, *mesotrophic* for lakes with intermediate productivity, and *eutrophic* for lakes with elevated productivity compared with the natural basic level. For this study, the class of atrophy is established based on phosphorous only, to facilitate mathematical modeling. However, levels of phosphorous do not appear in the Streeter-Phelps formulations. A ratio was therefore used relating phosphorous to BOD. In a first step, the organic loads discharged into reservoirs were calculated based on the node-link network. DOCEAN/UFPE (2001) in a study for the Alto Pirapama cite a ratio of $BOD/P_0 = 58$ and state that 10 percent of the organic value would be subject to oxidization. In our case study, cane residue can be considered the sole polluting source due to fertirrigation. The ratio cited in the study was used to convert the BOD load discharge into a phosphorous load discharge into reservoirs. In a second step, maximum load levels to avoid eutrophication were determined using the model of Vollenweider (1976) cited in Von Sperling (1996). It allows the estimation of the concentration as a function of the affluent load, time detained, and geometrical characteristics. The model was drawn up for temperate lakes but has been adapted to tropical lakes by Salas and Martino (1991), also quoted by Von Sperling (1996). Thus, the maximum admissible phosphorous loading is established by the following expression:

$$L = P.V. \left(\frac{1}{t} + \frac{2}{\sqrt{t}} \right) \quad (11)$$

where L is the affluent load of phosphorous (ton P/month), P is the concentration of phosphorous in the lake (gP/m^3), V is the volume of the reservoir (million m^3), and t is the time of hydraulic detention (month). An estimate of t quoted by Von Sperling (1996) is used and given as

$$t = \frac{V}{Q} \quad (12)$$

where Q is the average affluent runoff in millions of cubic meters per month. Next, the time of hydraulic detention was calculated for each reservoir.

To determine the maximum admissible load, it would still be necessary to determine the lowest concentration of phosphorous above which the lake may be considered eutrophic. The band of phosphorous concentration in a eutrophic body of water, found in the references, is 0.025 to 0.1 grams of phosphorus per cubic meter gP/m^3 . Fixing an ideal value, whether more relaxed or restrictive, for

phosphorous must be done case by case, after analyzing the multiple uses of the dam and their degrees of importance. For the study, the most restrictive value was used for the two dams of the model, namely 0.025. Therefore, the inequality used in the model to restrict the affluent load of phosphorous (and thus discharged organic loads) into the reservoirs is given by

$$L * \frac{1}{V(\frac{1}{t} + \frac{2}{\sqrt{t}})} \leq 0.025 \quad (13)$$

Integration of Water Quantity and Quality Components in the Optimization Model

The water quantity and quality components were integrated in a river basin model, which was developed as a node-link network with underlying nodes and links including source nodes, which represent physical entities such as rivers and reservoirs, and demand nodes, including agroindustries, towns, and small hydroelectric stations (Figure 2). Effluent supply and demand nodes are defined for the areas planted with fertirrigated sugarcane, and effluent discharge from the irrigated land is assumed to be in proportion to fertirrigated areas.

Model Solution and Data Used

The model is highly nonlinear, particularly regarding equations on water quality. The number of nonzero and nonconstant elements in the Jacobian matrix serves as a measure of the nonlinearity of the model. Here, 33 percent of the nonzero elements in the Jacobian are nonconstant. With more than 10,000 variables and restrictions, the model can be considered in the category of large and complex nonlinear systems.

To solve the model, the piece-by-piece approach presented in Cai et al. (2001) was used. The solution for a submodel is used as a starting point for the following submodel. The water quantity submodel was run first (submodel 1) followed by the water quality model (submodel 2). Submodel 1 focuses on mass balances and water quantity allocations, whereas submodel 2 uses these allocations as a starting point to calculate pollution concentrations and the transport of modeled quality constituents and reservoir loads. The objective of the second submodel is to maximize basin net benefits subject to both water quantity and quality constraints, to reflect current legislation and to prevent reservoir eutrophication.

The data used in the river basin model include hydrologic data simulating the water supply side along the water course, economic data to develop water demand and net benefit functions, and physical data such as cross-section areas for the river bed and segment length needed for the water quality equations. Economic data collected include average water delivery costs, autonomous consumption (Q_0 in equation 1), that is, the amount of water allocated to a specific user for which no positive value can be attributed. For instance, in a small central hydroelectric (SCH), water flows that exceed installed capacity for power generation have no value for the user. For the case of domestic consumption, the maximum water main capacity represents autonomous consumption. Net benefits associated with specific water allocations for each of the users and values of the price elasticity for the various uses were obtained from the literature, field work, and user interviews.

Data for the water quality model include both physical data and parameters that simulate the river's autodepuration processes such as coefficients of deoxygenation and reaeration. Physical data were obtained from a prior river bathymetric survey (DOCEAN/UFPE 2001). Some parameters were obtained from measurements taken at quality stations for the base year, for example, for monthly values of saturated dissolved oxygen (DO_{sat}).

Process parameters were mostly obtained from the literature (Von Sperling 2006) based on specific physical characteristics. For instance, the aeration coefficient is tabled as a function of river velocity. The velocity is a function of the cross-sectional area and water flow in a specific stretch. Water

flow again is a function of water allocation to various users and uses and thus codetermines the river autodepuration capacity.

3. ANALYSIS OF RESULTS

The results from submodel 1, called submodel from now on, are first described and compared with the de facto water allocation and fertirrigation practices in the basin. Then the results from submodel 2, the full model, are compared with the submodel; and implications for water quality regulations for fertirrigation, effluent reuse, and reservoir operations are discussed.

Submodel Results

With a normal hydrologic year in the basin, the submodel results indicate a slight decline in hydropower generation (less than 1 percent for SHSCIP) and full water supply to other sectors. To test water allocation principles, the model was applied to a dry scenario with 60 percent of normal flow in each month. The results are presented in Table 1. Under low-flow conditions, only the agroindustries JB, Sibéria, and Liberdade can have full water supply. Economic losses are significant for hydropower (10.7 percent for SHSCIP and 1.3 percent for SHSJB, as a result of water allocation reductions of 20.6 percent and 3.3 percent, respectively), and minor for municipal water supply for Vitória and Recife. Different levels of economic losses can be explained by the variations in net marginal benefits for different water-use sectors. The agroindustries are fully served since the net marginal benefit is the highest. The water demand for the SHSCIP power plant competes with demand from the JB distillery and the municipality of Vitória, which both have higher net marginal benefits than SHSCIP. The flow reduction at SHSJB occurs only during the harvest period, coinciding with a dry month, in which water demand for SHSJB competes with that for the JB distillery.

Table 1. Submodel 1 water allocation results under low-flow scenario (60% of average flows)

Water users	Monthly flow demand ^a (m ³ /s) Q_{req}	Avg. monthly flow supplied ^c (m ³ /s)	Avg. cost ^a (US\$/ m ³) CW	Raw water loss ^a percentage	Demand- price elasticity ^a η	Autonomous consumption ^b (m ³ /seg) Q_0	Price at rationing (US\$/m ³) ^b P_0	Avg. net marginal benefits ^d in US\$/m ³ $(\frac{P_1 - C_{med}}{2})$
Recife	5.120	5.118	0.4192	45	0.13	184.98	0.520	0.050
Vitória	0.119	0.117	0.4192	45	0.13	4.056	0.520	0.050
JB	0.433	0.433	0.4852	20	0.99	0.723	3.943	1.729
Sibéria	0.060	0.060	0.4852	20	0.99	0.075	2.194	0.854
Liberdade	0.370	0.370	0.4852	20	0.99	0.505	3.017	1.266
SHSJB	0.684	0.662	0.0011	0	0.28	1.577	0.008	0.003
SHSCIP	1.887	1.497	0.0008	0	0.28	4.351	0.006	0.002

^aData obtained from users and used in the construction of the inverse demand function.

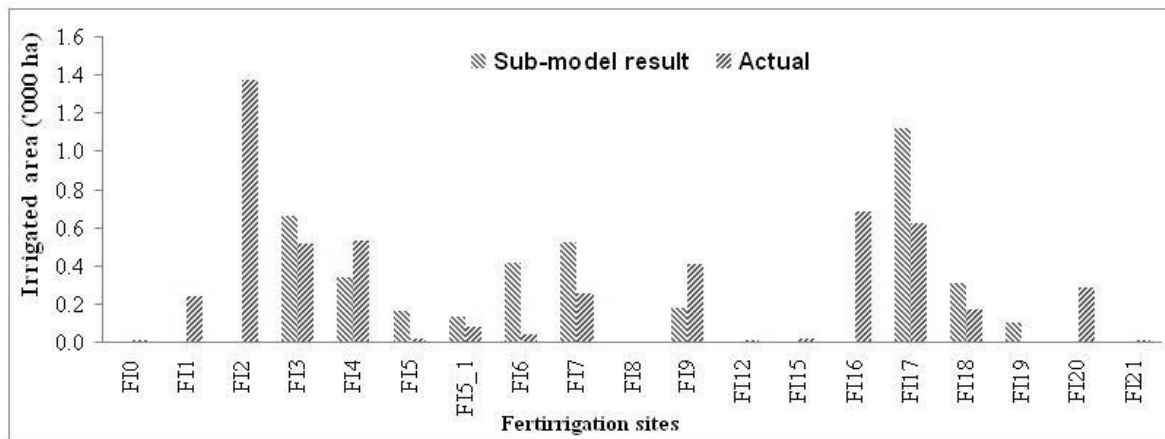
^b Values for autonomous consumption and price at rationing are determined according to equation (1).

^c The optimal allocated value is the average of optimal monthly results Q_a of submodel 1 under low flow.

^d Measure of the average net benefits of each user per cubic meter, from P_0 and CW.

Figure 4 compares modeled fertirrigated areas with actual areas assessed based on field interviews. Modeled fertirrigated areas reflect the optimal allocation of effluents produced by the agroindustries in the basin subject to maximizing economic benefits from fertirrigation and other sectors. Under optimized allocation, effluents are not located in demand sites that are far from distilleries due to high transportation costs. These include FI0, FI1, FI2, FI8, FI10, FI11, FI12, FI13, FI15, FI16, FI20, FI21, and FI23_1 (see also Figure 2). The optimal fertirrigated area is 68 percent of the total sugarcane area, excluding those areas with high transportation costs. Due to the limited total amount of effluents produced by the agroindustries, however, not all areas can be supplied. The agroindustries JB and Liberdade are close to effluent demand sites and supply sufficient crop residues without high transportation costs. The Sibéria distillery, on the other hand, produces a relatively small volume of effluents. As a result, the share of fertirrigated area is 57 percent for the demand sites in JB (FI3–FI7), and 62 percent for the fertirrigation sites in Liberdade (FI17–FI19). In Sibéria, only demand site FI9 receives the whole effluent requirement demanded, and the fertirrigated area covers 13 percent of the total area in Sibéria. Within one district (areas fertirrigated by one distillery), the share of fertirrigated area is the same for all demand sites, because it is assumed that crop productivity and costs are the same.

Figure 4. Actual and fertirrigated areas compared with modeled areas in the submodel with 60 percent of normal hydrology (dry scenario)



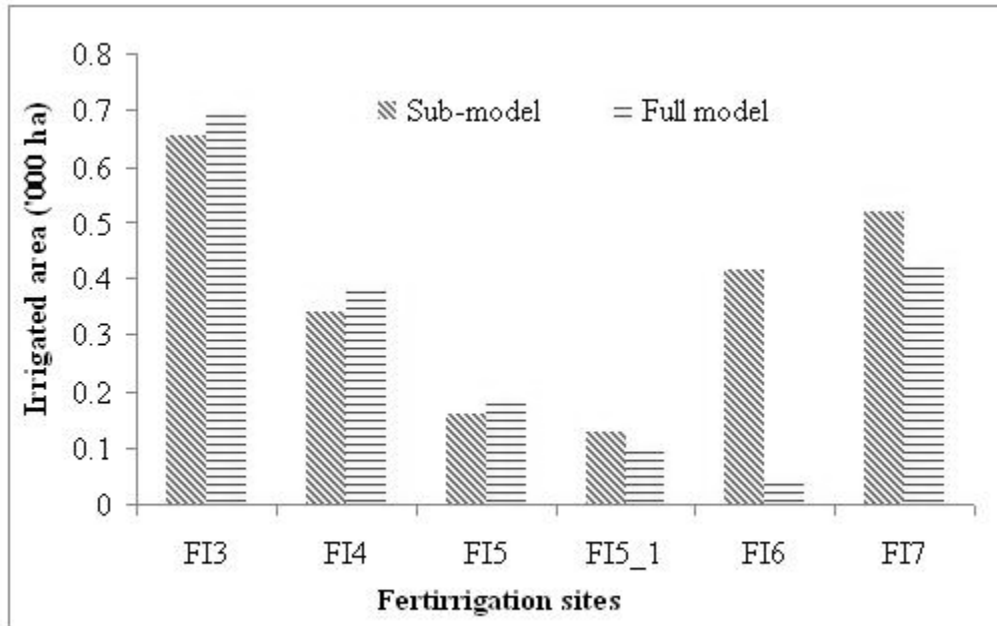
Comparison of Results from Submodel and Full Model

The full model with water quality restrictions results in a decrease in net benefit for all uses by 0.7 percent compared with the quantity submodel. Fertirrigation loses 10 percent and agroindustries 0.25 percent. This implies that the use of vinasse has a significant impact on water quality and provides significant economic benefit. The agroindustry JB suffers an economic loss of 0.50 percent compared with the results from the submodel, because the effluent produced by JB is not completely applied through fertirrigation, requiring effluent surplus treatment and transportation to maintain water quality constraints.

Compared with the results of the submodel, some fertirrigated areas gain and others lose when water quality constraints are enforced. An example is shown in Figure 5 for district JB. Demand sites FI5_1, FI6, and FI7 have a drainage rate about 3.5 times the level of FI3, FI4, and FI5. In the full model, 57 percent of the effluent produced in JB is applied to FI3, FI4, and FI5, and only 26 percent to FI5_1, FI6, and FI7; 18 percent is leftover. Vinasse applications to FI6 are particularly low, cutting off most of the fertirrigated area in the demand site. FI6 is located upstream of the Águas Claras reservoir (Figure 2), and water quality in the reservoir is very sensitive to the discharge of organic matters from FI6. Moreover, the effluent allocation among the demand sites is affected by dilution flow requirements in order to maintain an appropriate DO level in the river reaches. This is because besides the allocated load (BOD₀), pollution levels at river reaches are determined by the dilution flow, which is a function of the

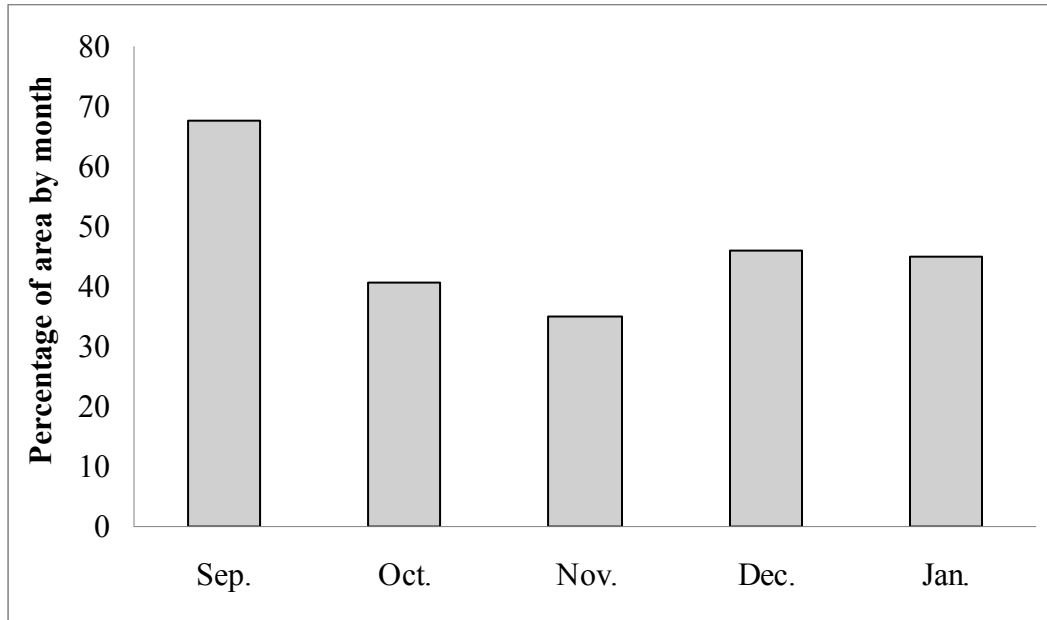
water level and depends on offtakes in that stretch and the downstream reservoir. Thus, with water quality restrictions, the vinasse allocation among demand sites depends on the location of the site with respect to its drainage generation rate, the specific dilution requirement flows to maintain DO levels, and the location relative to reservoirs.

Figure 5. Fertirrigated areas for JB in submodel 1 and the full model.



The impact of water quality restrictions can be further examined by the monthly distribution of fertirrigation applications in a demand site. Using FI7 in JB as an example, the water quantity submodel results in the same fertirrigated area over all sugarcane growing months, about 57 percent of total area. When water quality constraints are introduced, the fertirrigated area declines to a monthly average of 47 percent of total area. Moreover, area can change across months based on runoff. For example, in September, 68 percent of the total area is fertirrigated, but fertirrigated area shrinks to 46 percent of the sugarcane area in December. In general, fertirrigated areas decline in months with lower flow volumes because fewer flows are available for effluent dilution. On the other hand, lower runoff also results in lower runoff from fields, which explains why fertirrigated area is not smallest in the months with lowest flows (December and January; see Figure 6).

Figure 6. Fertirrigated areas as a share of total area in node FI7, full model



Similarly, the monthly BOD loads do not fully correspond with the expansion of fertirrigated areas (Figures 6 and 7). BOD loads during October, December, and January are lower as a result of reduced runoff. Since the dilution flow considered in the equations of organic compounds decay is the minimum at the stretch, reduction in allocated loads (reduction in vinasse application that is the major contributor to BOD loads) seems to be the most important strategy to meet quality restrictions.

Figure 7. BOD loads in thousands of Kg BOD/day, site FI7, full model

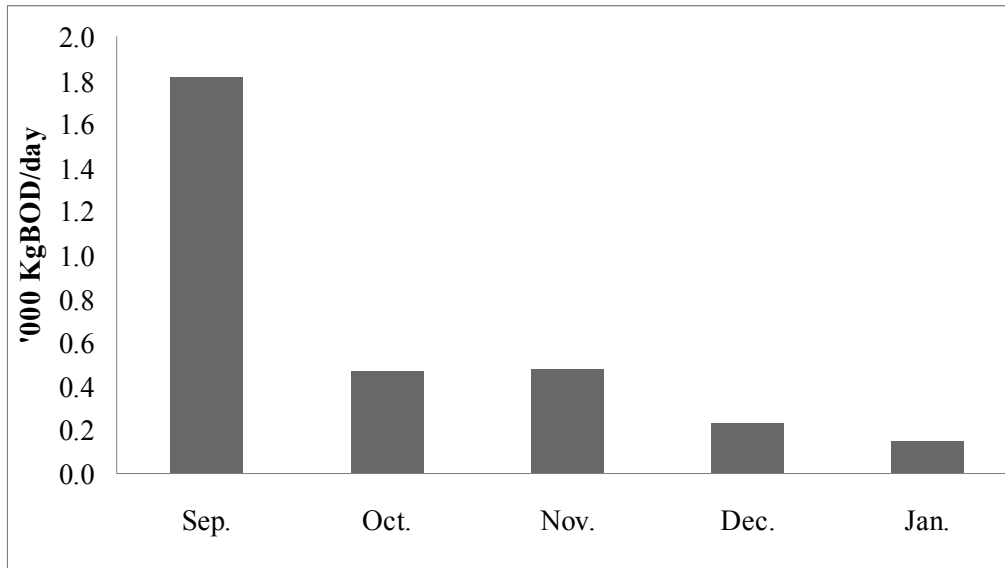


Figure 8 presents changes in water supply to Vitória under the submodel and the full model as well as the city's water use right (flow demand). As can be seen, with the combined water quantity/quality model, domestic water supply of Vitória cannot be fully met in the months of September

to February because of water quality constraints. Moreover, the flow release from the Águas Claras reservoir to the SHSCIP hydropower station will be reduced. Water supply reductions are due to low flows (December and January) and sugarcane harvesting periods, except for September, to maintain requirements for the Águas Claras reservoir and dilution flows for river reaches downstream of Vitória. Dilution flows are required due to runoff from fertirrigation at sites FI5, FI5_1, FI6, and FI7 from district JB, upstream and downstream of Vitória (see Figure 2). Figure 9 presents the BOD loads from fertirrigation demand sites. Even though loads are highest in September, natural flows are also largest in that month. Thus, there is no need for reserving flow for dilution in that month.

Figure 8. Water allocation for Vitória resulting from the submodel and full model and water use right (=flow demand).

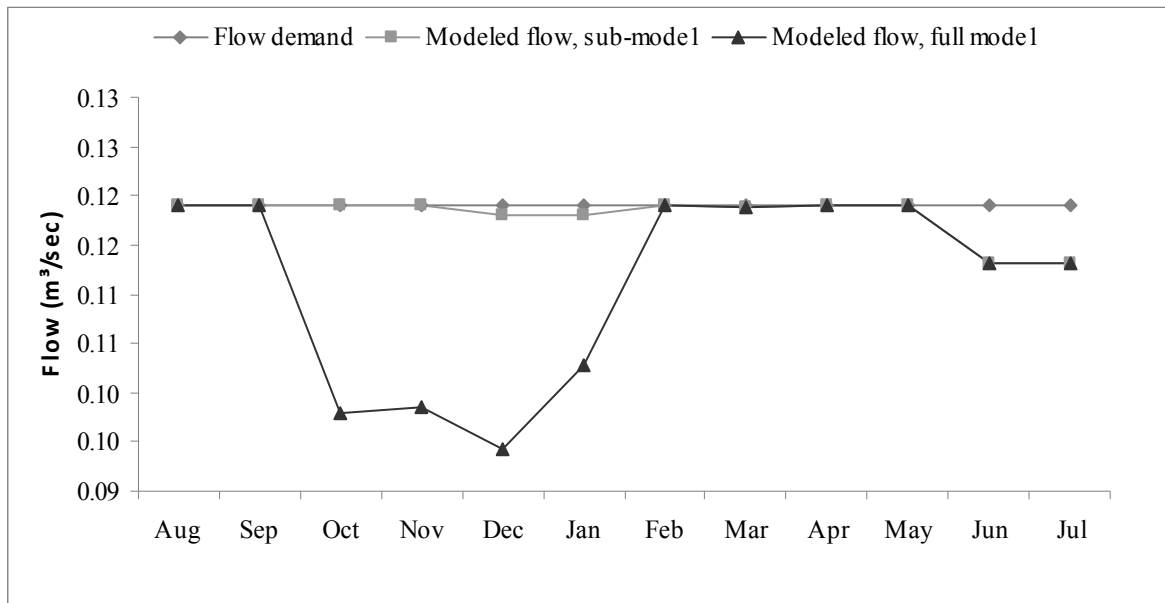
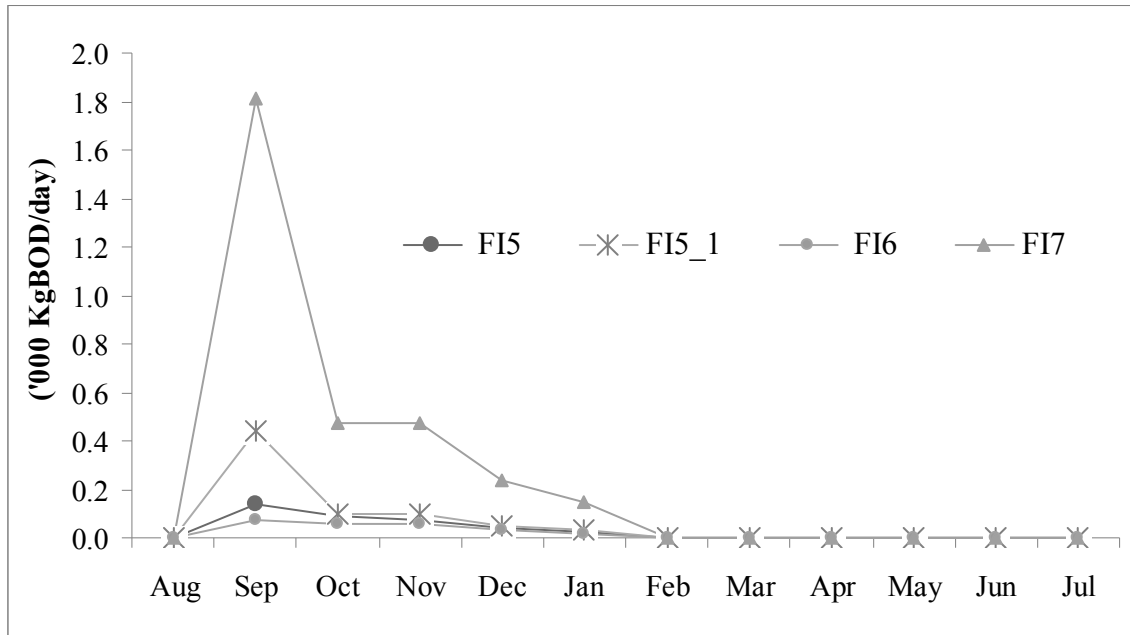


Figure 9. BOD loads with the full model for fertirrigated sites: FI5, FI5_1, FI6, and FI7



The reductions of water supply to Vitória and the hydropower station SHSCIP are related to the relative location of Vitória, SHSCIP, and JB (Figure 2). With water quality constraints in place, a tradeoff exists among the economic benefits from the agroindustry, hydropower generation, and municipal water supply. Reductions of municipal water supply and flow discharge to the hydropower station are traded with benefits from agroindustrial use. According to the marginal economic values for different distilleries and cities (Table 1), JB has a higher marginal value than Vitória’s municipal water supply. Thus, the water supply reductions for Vitória are not only due to water quality constraints, but also to the objective of maximizing the net benefits to water use in the basin.

The relationship between the Águas Claras reservoir and the SHSCIP hydropower station merits further discussion. A reduction of water supply to Vitória increases flow dilution downstream of the reservoir and helps maintain sufficient reservoir storage to prevent eutrophication. As shown in Figures 10 and 11, in the month of December the full model results in lower reservoir storage and higher releases, increasing the flow for electricity generation; and in the dry month of January, the situation is reversed. The shadow price for storage to prevent eutrophication, which is highest in September and January, helps explain this situation (Figure 12). The shadow prices can be used to infer the cost of pollution prevention measures or economic incentives such as pollution taxes, which could vary by month. Nonzero shadow prices imply that the constraint related to reservoir water quality is binding and that a tradeoff exists between water quality and water supply. More research is necessary to determine how such a pollution tax could be implemented.

Figure 10. Águas Claras reservoir storage from the submodel and full model

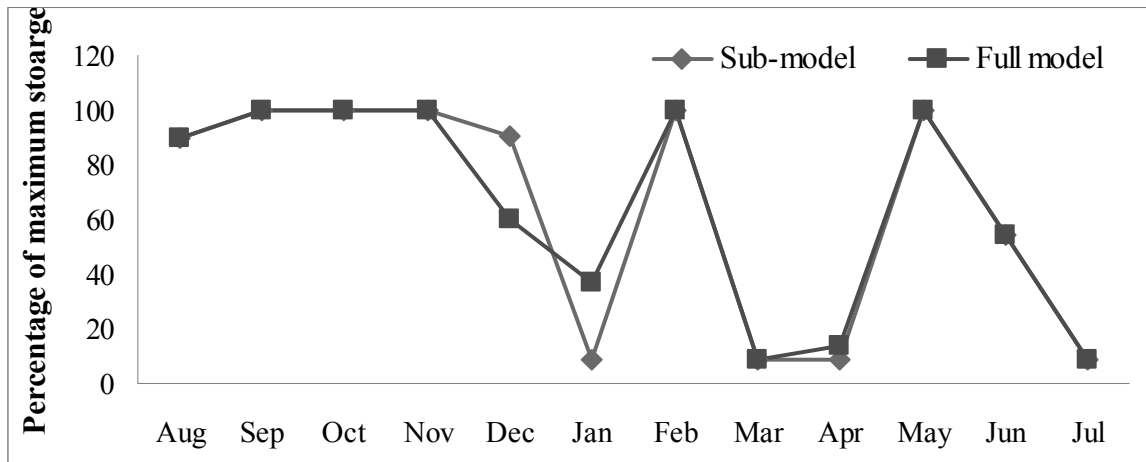


Figure 11. Flow release from Águas Claras reservoir under the submodel and the full model

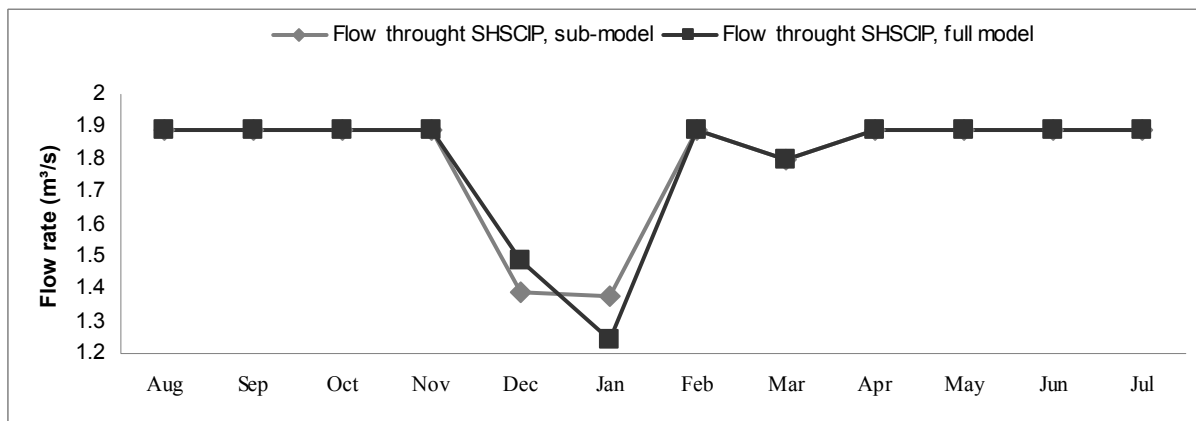
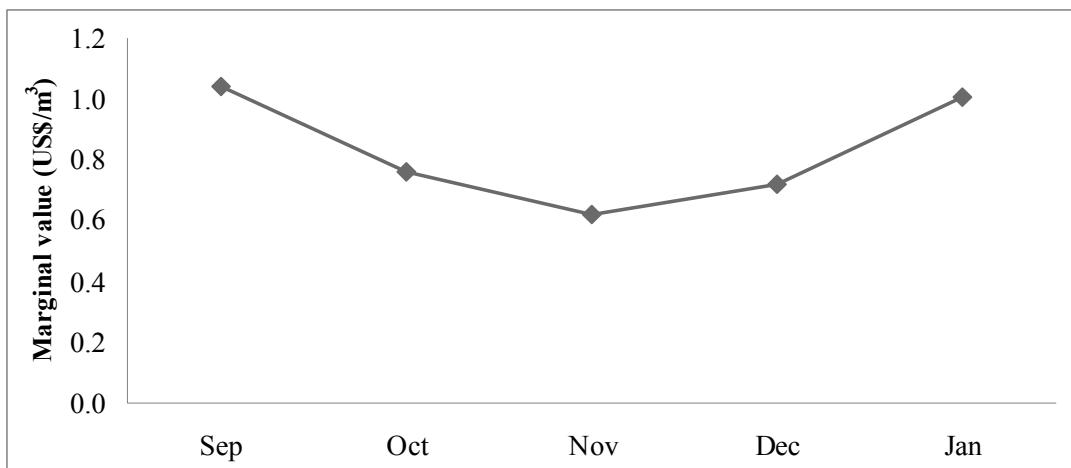


Figure 12. Shadow-price on the limit of phosphorus for Águas Claras reservoir, full model



4. CONCLUSIONS

This paper presented a combined water quantity/quality model for an important sub-basin of the Pirapama River to study the impact of enforced water pollution standards on fertirrigation. Fertirrigation is becoming increasingly important for Brazil given that the demand for bioethanol from sugarcane has skyrocketed in recent years, and combined water quantity/quality modeling can yield important insights on tradeoffs between the costs of reduced water quality compared with the benefits of increased vinasse application.

The model's main advantage is its ability to reflect the interrelationships between essential hydrologic, agronomic, and economic components and to explore both economic and environmental consequences of various policy choices. Results for the water quantity model show that without water quality constraints almost all water demands can be met, even during harvest months. If water quality restrictions are introduced, however, net benefits are significantly reduced, particularly for industrial water use and fertirrigation. With water quality constraints, the largest agroindustry no longer allocates all effluents to sugarcane areas due to high transportation costs, even though the nonallocated residues need to be treated to reduce adverse environmental impacts. Net benefits also decline for other water users as water quality restrictions require higher instream flows for flow dilution and increased reservoir storage to avoid eutrophication. To enforce water quality restrictions, the shadow price for maintaining water in the reservoir could be used as a pollution tax for fertirrigated areas, which are currently not subject to pollution charges. Further research will be necessary to study this issue in detail. Additional analyses can also be undertaken to examine the impact of alternative water and pollution charges on fertirrigated areas.

REFERENCES

- Cai, X., D. McKinney, and L. A. Lasdon. 2001. Piece-by-piece approach to solving large non-linear water resources management models. *Journal of Water Resources Planning and Management* 127: 363–368.
- Cai, X., D. McKinney, and L. A. Lasdon. 2003. Integrated hydrologic-agronomic-economic model for river basin management. *Journal of Water Resources Planning and Management* 129 (1): 4–17.
- Cai, X., M. W. Rosegrant, and C. Ringler 2006. *Modeling water resources management at the basin level: Methodology and application to the Maipo River Basin*. Research Report 149. Washington, D.C.: International Food Policy Research Institute.
- Carrera-Fernandez, J. 1999. *Estudo de Cobrança pelo uso da água na bacia hidrográfica do Rio Pirapama*. Casa Forte, Recife, Pernambuco, Brazil: CPRH.
- DFID (Departament for Internacional Development) and CPRH (Companhia Pernambucana do MeioAmbiente). 1999. *Diagnóstico Ambiental Integrado da Bacia do Pirapama*. Casa Forte, Recife, Pernambuco, Brazil: CPRH.
- DOCEAN/UFPE (Universidade Federal de Pernambuco). 2001. *Estudos da Dinâmico do Alto Pirapama montante da futura represa*. Departamento de Oceanografia. Recife, Pernambuco, Brazil:UFPE.
- Gama, A.M.F. (ed.). 1998. *Estudo da qualidade de água da bacia do rio Pirapama*. Casa Forte, Recife, Pernambuco, Brazil: CPRH.
- International Sugarcane Biomass Utilization Consortium. 2007. Vinasse: Life cycle analysis and cost assessment of different methods for its disposal. International Sugarcane Biomass Utilization Consortium. <<http://issct.intnet.mu/ISBUCresprop2.HTM>> Last accessed June 4, 2009.
- Loucks, D. P., C. S. Revelle, and W. R. Lynn. 1967. Linear programming models for water pollution control. *Management Science* 14 (Application Series): B166–B181.
- Ludovice, M.T.F., D. B. Vieira, and J. R. Guimaraes. 2005. *Infiltração de Vinhaça em Canal de Terra: Alteração de Teor de Matéria-orgânica e Sais no Solo e na Água*. Sao Paulo, Brazil: Sociedade Brasileira de Química.
- Moraes, M.M.G.A. de. 2003. Modelo econômico-hidrológico Integrado para Alocação Ótima de Água em Diferentes Usos em Áreas Plantadas de Cana na Bacia do Rio Pirapama. *Tese Doutorado*. Recife, Pernambuco, Brazil:UFPE.
- Moraes, M.G.A., Y. Sampaio, and J. A. Cirilo. 2006. Integração de componentes econômicos e hidrológicos na modelagem de alocação ótima de água para apoio a gestão de recursos hídricos: Uma aplicação na bacia do pirapama. *Revista Economia* 7 (2): 341-364.
- Ribeiro, M. 2000. Alternativas para a outorga e cobrança pelo uso da água. *Tese Doutorado*. Universidade Federal do Rio Grande do Sul (UFRGS), Porto Alegre, Rio Grande do Sul, Brazil: UFRGS.
- Salas, H. J., and P. Martino. 1991. A simplified phosphorus trophic state model for warm-water tropical lakes. *Water Research* 25 (3): 341-350.
- Streeter, H. W., and E. B. Phelps. 1925. A study of the pollution and natural purification of the Ohio River. *Public Health Bulletin* 146.
- Vollenweider, R. A. 1976. Advances in defining critical loading levels for phosphorus in lake eutrophication. *OECD Cooperative Programme in Eutrophication*: 55-83 .
- Von Sperling, M. 1996. *Introdução à qualidade das águas e ao tratamento de esgotos*. Pampulha, Belo Horizonte, Minas Gerais, Brazil: Universidade Federal de Minas Gerais (UFMG).

RECENT IFPRI DISCUSSION PAPERS

For earlier discussion papers, please go to www.ifpri.org/pubs/pubs.htm#dp.
All discussion papers can be downloaded free of charge.

866. *Economywide economic impact of Avian flu in Ghana: A dynamic CGE model analysis*. Xinshen Diao, 2009
865. *Brazil: Shadow WTO agricultural domestic support notifications*. Andre M. Nassar and Diego Ures, 2009.
864. *HIV/AIDS, growth and poverty in KwaZulu-Natal and South Africa: Integrating firm-level surveys with demographic and economywide modeling*. James Thurlow, Gavin George, and Jeff Gow, 2009.
863. *The short-run macroeconomic impact of foreign aid to small states: an agnostic time series analysis*. Henrik Hansen and Derek Headey, 2009.
862. *European Union preferential trade agreements with developing countries and their impact on Colombian and Kenyan carnation exports to the United Kingdom*. Guylain K. Ngeleza and Andrew Muhammad, 2009
861. *The linkages between agriculture and malaria: Issues for policy, research, and capacity strengthening*. Kwadwo Asenso-Okyere, Felix A. Asante, Jifar Tarekegn, and Kwaw S. Andam, 2009.
860. *La biotecnología agropecuaria en América Latina: Una visión cuantitativa*. José Falck-Zepeda, César Falcón, María José Sampaio-Amstalden, José Luis Solleiro Rebolledo, Eduardo Trigo, and Javier Verástegui, 2009.
859. *Preferential trade agreements between the monetary community of Central Africa and the European Union: Stumbling or building blocks? A general equilibrium approach*. Guylain K. Ngeleza and Andrew Muhammad, 2009.
858. *Preliminary evidence on internal migration, remittances, and teen schooling in India*. Valerie Mueller and Abusaleh Shariff, 2009.
857. *Productivity convergence in Brazil: The case of grain production*. Eduardo Magalhaes and Xinshen Diao, 2009.
856. *Dynamics of structural transformation: An empirical characterization in the case of China, Malaysia, and Ghana*. Thaddee Badibanga, Xinshen Diao, Terry Roe, and Agapi Somwaru, 2009.
855. *Do institutions limit clientelism? A study of the district assemblies common fund in Ghana*. Afua Branoah Banful, 2009.
854. *The evolution of Chinese entrepreneurial firms: Township-village enterprises revisited*. Chenggang Xu and Xiaobo Zhang, 2009.
853. *Evaluating the impact of land tenure and titling on access to credit in Uganda*. Carly K. Petracco and John Pender, 2009.
852. *Participation by Men and Women in Off-Farm Activities: An Empirical Analysis in Rural Northern Ghana*. Nancy McCarthy and Yan Sun, 2009.
851. *Measuring agricultural innovation system properties and performance: Illustrations from Ethiopia and Vietnam*. David J. Spielman and Dawit Kelemework, 2009.
850. *Are returns to mothers' human capital realized in the next generation?: The impact of mothers' intellectual human capital and long-run nutritional status on children's human capital in Guatemala*. Jere R. Behrman, Alexis Murphy, Agnes R. Quisumbing, and Kathryn Yount, 2009.
849. *Understanding Farmers' Perceptions and Adaptations to Climate Change and Variability: The Case of the Limpopo Basin, South Africa*. Glwadys Aymone Gbetibouo, 2009.
848. *Agglomeration, migration, and regional growth: A CGE analysis for Uganda*. Paul Dorosh and James Thurlow, 2009.
847. *Biosafety decisions and perceived commercial risks: The role of GM-free private standards*. Guillaume Gruère and Debdatta Sengupta, 2009.
846. *Impact of soaring food price in Ethiopia: does location matter?* John M. Ulimwenju, Sindu Workneh, and Zelekawork Paulos, 2009.
845. *Aggregate effects of imperfect tax enforcement*. Miguel Robles, 2009.
844. *Agricultural strategy development in West Africa: The false promise of participation?* Danielle Resnick and Regina Birner, 2008.

**INTERNATIONAL FOOD POLICY
RESEARCH INSTITUTE**

www.ifpri.org

IFPRI HEADQUARTERS

2033 K Street, NW
Washington, DC 20006-1002 USA
Tel.: +1-202-862-5600
Fax: +1-202-467-4439
Email: ifpri@cgiar.org

IFPRI ADDIS ABABA

P. O. Box 5689
Addis Ababa, Ethiopia
Tel.: +251 11 6463215
Fax: +251 11 6462927
Email: ifpri-addisababa@cgiar.org

IFPRI NEW DELHI

CG Block, NASC Complex, PUSA
New Delhi 110-012 India
Tel.: 91 11 2584-6565
Fax: 91 11 2584-8008 / 2584-6572
Email: ifpri-newdelhi@cgiar.org